Journal of Applied Physics

Cadmium trapping by C_{60} and B-, Si-, and N-doped C_{60}

Cite as: J. Appl. Phys. **125**, 054302 (2019); https://doi.org/10.1063/1.5080351
Submitted: 07 November 2018 . Accepted: 23 January 2019 . Published Online: 07 February 2019

Navaratnarajah Kuganathan, Namasivayam Selvanantharajah, Poobalasuntharam Iyngaran, Poobalasingam Abiman, and Alexander Chroneos

Journal of Applied Physics ARTICLE scitation.org/journal/jap

Cadmium trapping by C_{60} and B-, Si-, and N-doped C_{60}

Cite as: J. Appl. Phys. **125**, 054302 (2019); doi: 10.1063/1.5080351
Submitted: 7 November 2018 · Accepted: 23 January 2019 ·
Published Online: 7 February 2019

Navaratnarajah Kuganathan,[1,a)] Namasivayam Selvanantharajah,[2] Poobalasuntharam Iyngaran,[2] Poobalasingam Abiman,[2] and Alexander Chroneos[1,3,a)]

AFFILIATIONS

[1]Department of Materials, Imperial College London, London SW7 2AZ, United Kingdom
[2]Depratment of Chemistry, University of Jaffna, Sir Pon Ramanathan Road, Thirunelvely, Jaffna, Sri Lanka
[3]Faculty of Engineering, Environment and Computing, Coventry University, Priory Street, Coventry CV1 5FB, United Kingdom

[a)]**Authors to whom correspondence should be addressed:** n.kuganathan@imperial.ac.uk and alexander.chroneos@imperial.ac.uk

ABSTRACT

The removal of heavy metals from the environment has attracted considerable attention as they are toxic and non-biodegradable or destroyable. To minimize their hazard, they should be removed through either physical or chemical capture. Cadmium is a heavy metal that can lead to severe risks to human health. Using the density functional theory with a dispersion correction (DFT + D), we predict the structures and energies of Cd trapped by C_{60}. Furthermore, we substitutionally doped C_{60} with a single B, Si, and N and examined its trapping behavior. The lowest substitutional energy was calculated for B. Significant enhancement in trapping is observed with B and Si doping outside the surface in particular and our results warrant further experimental investigation.

I. INTRODUCTION

Rapid industrial usage of heavy metals such as cadmium, lead, copper, zinc, and mercury pollutes the environment directly or indirectly. Industrial activities, such as electroplating, smelting, mining, and manufacturing batteries and fertilisers, increase the level of toxic heavy metals in the aqueous environment with the possible risk of damaging human physiology.[1] As heavy metals cannot be biodegradable or destroyable unlike organic contaminants, its acceptable level of concentration exceeds and results in further damage to the environment.

Cadmium is one of the toxic heavy metals mainly found in cigarette smoke,[2] tap water,[3] and seafood.[4] Due to its very low excretion from the body, at a high level, it exposes human health to severe risks. It mainly damages the kidneys[5] and the cardiovascular system.[6] Thus, there is a necessity to remove cadmium, especially from water and air. Significant effort has been devoted to find ways to remove heavy metals using methods such as ion exchange,[7] solvent extraction,[8] coagulation,[9] adsorption,[10] chemical precipitation, and reverse osmosis.[11] Several sorbents including activated carbon,[12] carbon nanotubes,[13] chemically modified carbon,[10] zeolites,[14] and biomass[15] have been studied experimentally to remove heavy metals from water.

The buckyball (C_{60}) or its modified form (e.g., doped C_{60}) is a candidate material to trap cadmium as it provides both inner and outer surface structures. In addition, its high resistance to external chemical attack, light weight, and high mechanical stability at high pressure and temperatures attract C_{60} as a potential sorbent.[16] There are experimental and theoretical studies on alkali metals,[17–19] alkali earth metals,[17,20] radioactive isotopes,[21,22] actinide metals,[23] non-metals,[24,25] noble gases,[18] transition metals,[26,27] rare earth metals,[28] and metal clusters.[19,27]

Using the density functional theory (DFT) together with dispersion corrections (DFT + D), the thermodynamic stability of cadmium with the inner and outer surface of C_{60} is investigated. Furthermore, B, Si, and N is substitutionally doped and the stability of Cd is discussed. The DFT calculations, in addition to giving structural information, provide the electronic structure and properties.

II. COMPUTATIONAL METHODS

Calculations were carried out using the spin-polarized mode of the DFT as implemented in the VASP[29,30] package. The exchange-correlation term was modeled using the generalized gradient approximation (GGA) parameterized by Perdew, Burke, and Ernzerhof (PBE).[31] In all cases, we have used a plane-wave basis set with a cut-off value of 500 eV. A further increase in the plane wave-basis set cutoff would increase the computational time. In our previous study,[18] we have tested that 500 eV is sufficient for the convergence. Structural optimisations were performed using a conjugate gradient algorithm[32] and the forces on the atoms were obtained via the Hellman-Feynmann theorem including Pulay corrections. In all optimized structures, forces on the atoms were smaller than 0.001 eV/Å and all the values in the atomic stress tensor were less than 0.002 GPa. All geometry optimisations were performed using a single k-point because C_{60} is treated as a molecule and additional k-points did not make any significant difference in total energy. A cubic supercell with a length of 20 Å was used for all configurations to ensure that adjacent structures do not interact (the largest linear dimension of a C_{60} molecule was 7.10 Å). One of the limitations of this methodology is the size of the supercell. The larger supercell means a large number of plane wave basis sets with high computational time. We define the encapsulation energy for single Cd atom trapping inside the cage and association energy for single Cd atom trapping outside the cage by the following equation:

$$E_{Enc/Assoc} = E(Cd - C_{60}) - E(C_{60}) - E(Cd), \quad (1)$$

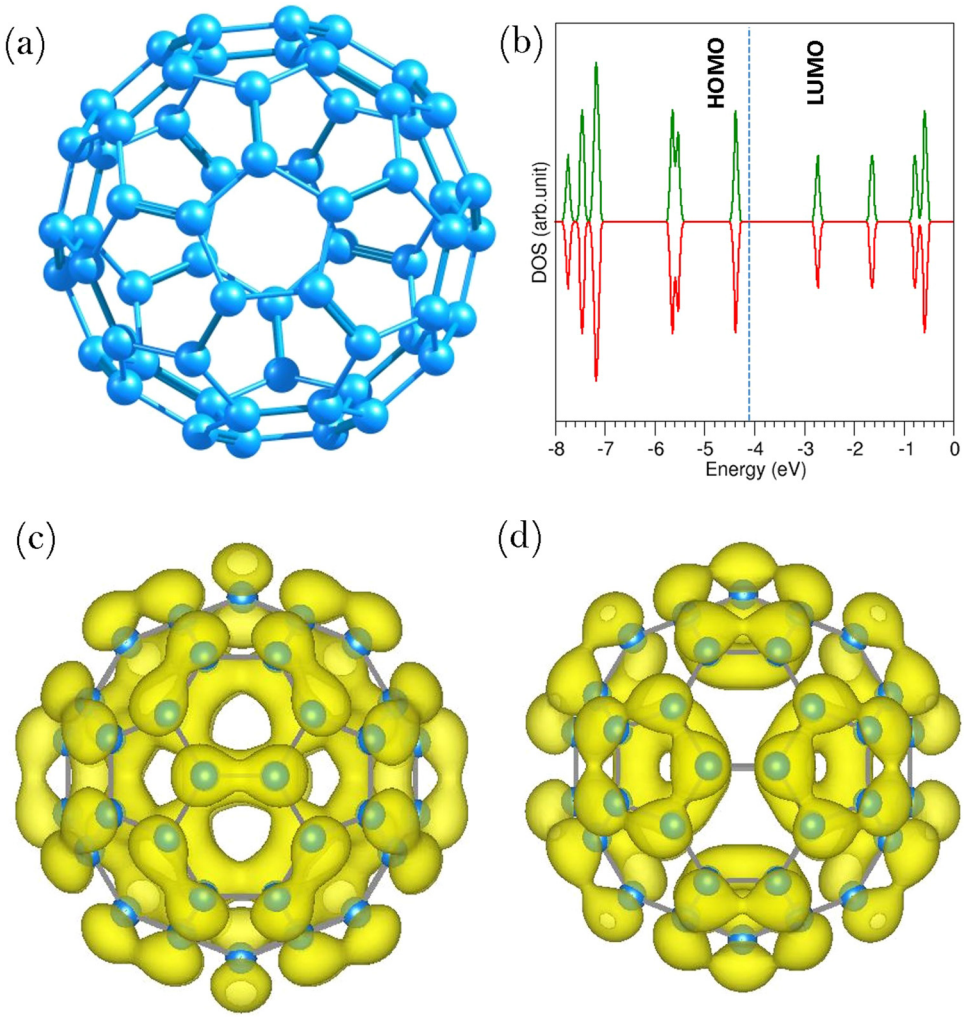

FIG. 1. (a) Relaxed structure of C_{60}, (b) total density of states of C_{60}, and (c) and (d) charge density isosurfaces of the HOMO and the LUMO, respectively. The vertical blue dotted line corresponds to the Fermi level.

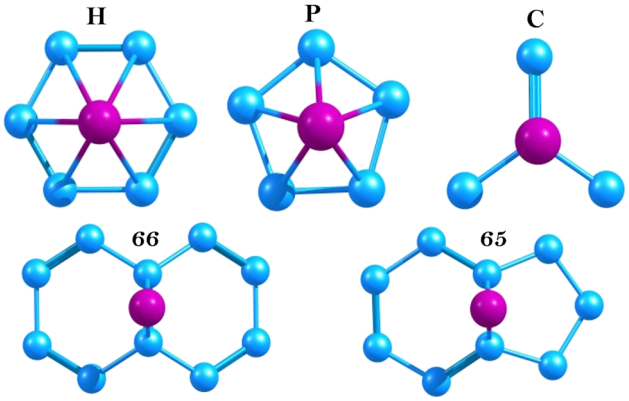

FIG. 2. Initial configurations of Cd absorbed exohedrally.

TABLE I. Initial and final configurations (refer to Fig. 2 for definitions) of Cd absorbed on C_{60} exohedrally and Bader charge on Cd atoms. The most stable configuration is highlighted in bold.

Initial configuration	Final configuration and relative association energy (eV)	Bader charge on Cd (|e|)
H	H, +0.02	+0.02
P	P, +0.04	+0.03
66	**66, +0.00**	+0.02
65	65, +0.04	+0.04
C	C, +0.05	+0.03

where $E(C_{60})$ is the total energy for the isolated C_{60} molecule, $E(Cd\text{-}C_{60})$ is the total energy of the Cd atom occupying the centre of the C_{60} cage or interacting on the surface of C_{60}, and $E(Cd)$ is the total energy of cadmium atom (the reference state).

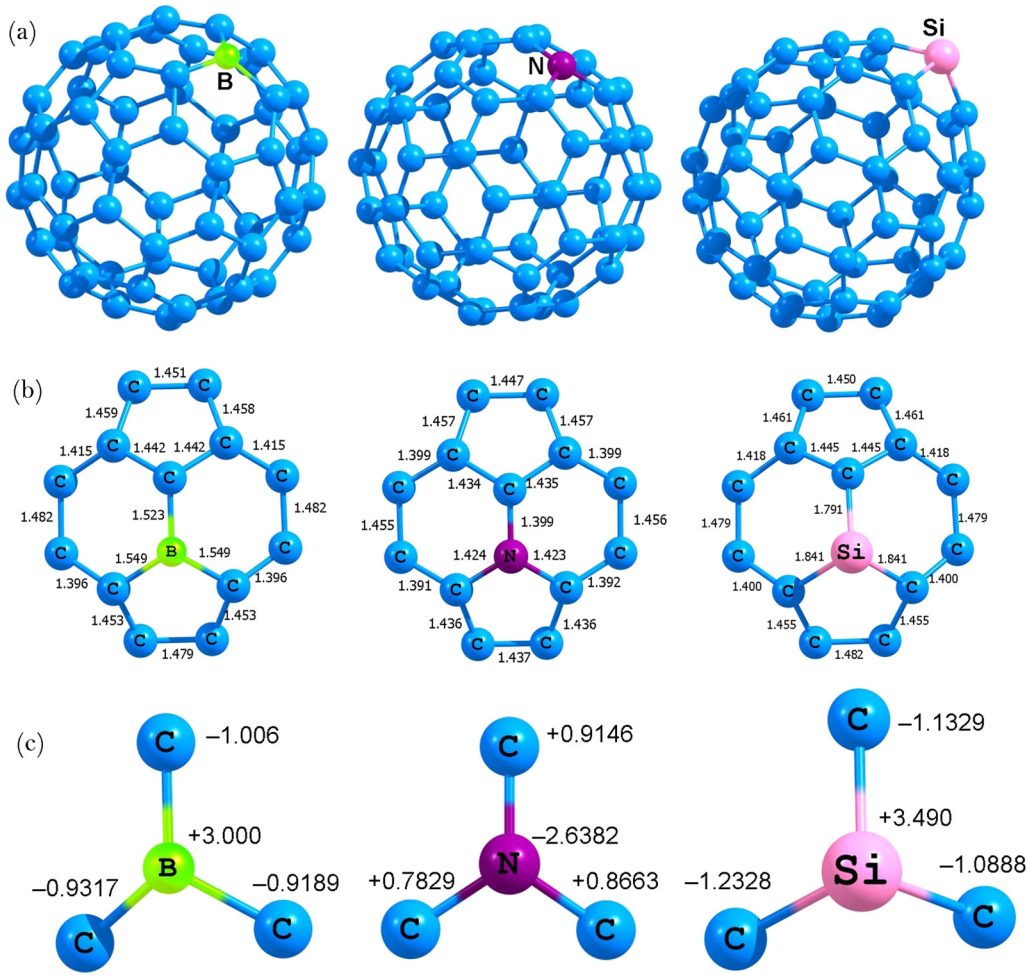

FIG. 3 (a) Relaxed structures B, Si, and N doped C_{60}, (b) bond distances closer to the dopants, and (c) Bader charges on dopants and their nearest neighbour carbons.

In order to calculate the encapsulation or association energy accurately, the dispersion has been included by using the pair-wise force field as implemented by Grimme *et al.*[33] in the VASP package.

All the calculations have been performed at isobaric conditions (P = constant) and thus no further thermodynamical corrections are necessary.[34] For example, the association energy depends on pressure and this has been well discussed by Varotsos.[34(a)]

III. RESULTS AND DISCUSSION

A. Structure and electronic properties of C_{60}

The starting point of the present study was to reproduce the experimental structure of C_{60} and compare its electronic structure with other theoretical studies to assess the quality of the pseudopotentials and basis sets used. Figure 1 represents the relaxed structure of C_{60}. In C_{60}, there are two different C—C bonds (C—C and C=C) present. The calculated bond lengths of C—C and C=C are 1.45 Å and 1.40 Å, respectively, in excellent agreement with corresponding experimental values of 1.43 Å and 1.39 Å.[35] The density of states (DOS) [refer to Fig. 1(b)] calculated for C_{60} predicts that the energy gap between the highest occupied molecular orbital (HOMO) [see Fig. 1(c)] and the lowest unoccupied molecular orbital (LUMO) [see Fig. 1(d)] is 1.55 eV, which is in good agreement with the value of 1.64 eV calculated by Goclon *et al.*[36]

B. Formation of Cd interacting with C_{60}

First, we consider the stability of Cd atom occupying inside the C_{60} cage. In the relaxed configuration, the position of the Cd atom remains very close to the centre of the cage. The encapsulation energy of Cd was calculated with and without dispersion and the corresponding encapsulation energy values are −0.18 eV and 0.55 eV, respectively, showing the necessity of including dispersion. Thus, in Secs. III C–III E, we only report the values calculated using dispersion.

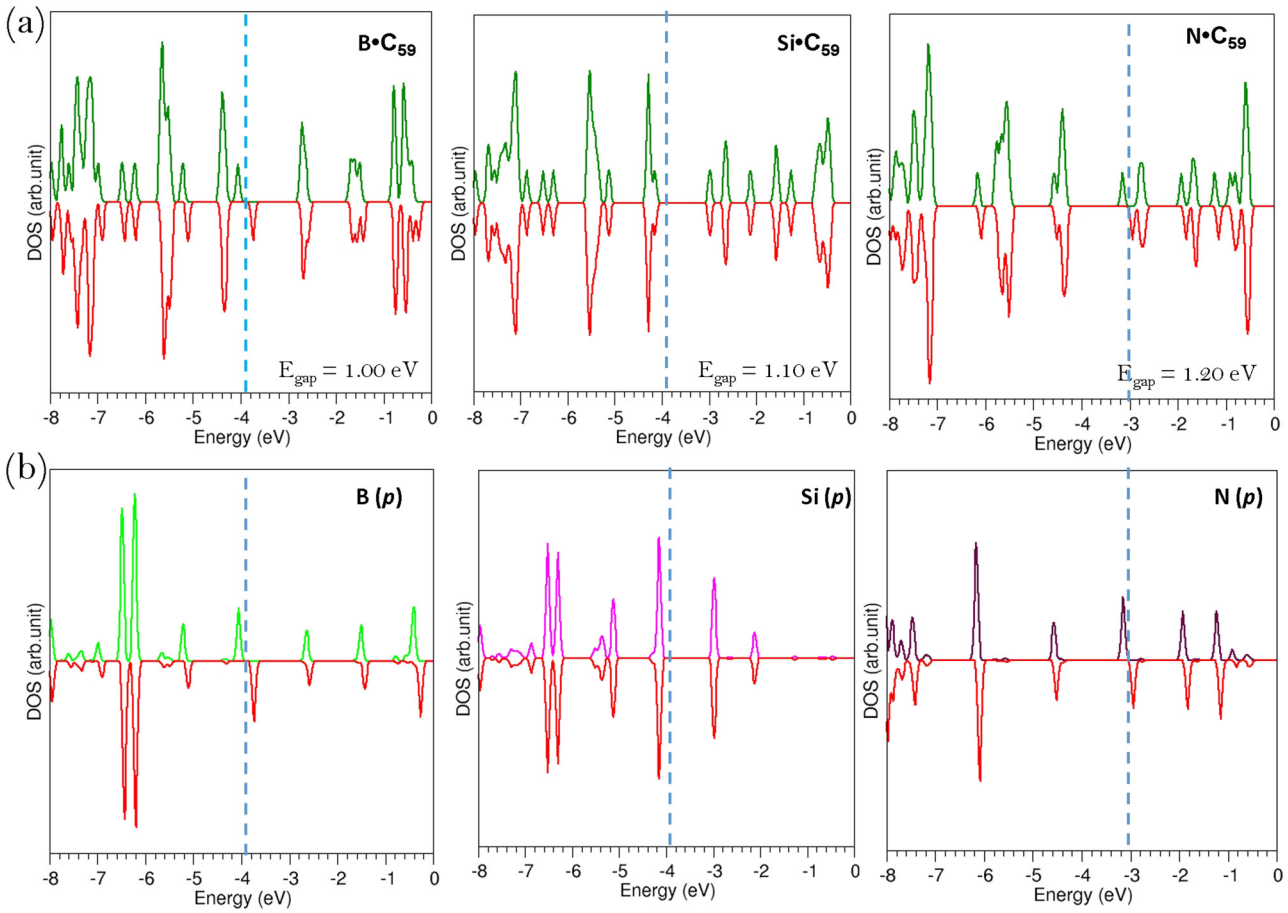

FIG. 4. (a) Total densities of states of doped C_{60} and (b) *p* states of doped atoms. The vertical dotted lines correspond to the Fermi energy level.

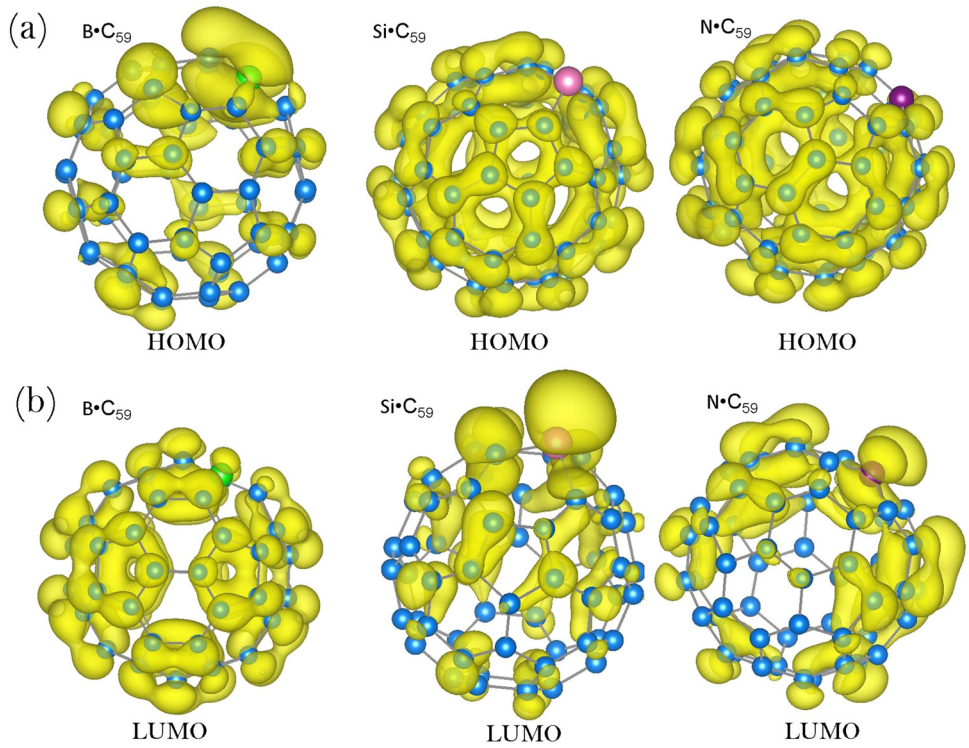

FIG. 5. (a) HOMO and (b) LUMO iso-surface charge densities calculated for C_{60} doped with B, Si, and N.

The encapsulation of Cd is exothermic with non-covalent nature. This is further supported by a small amount of charge transfer (0.10 |e|) from Cd to C_{60} according to the Bader charge analysis.[37]

Next, we considered the outer surface of the C_{60} for the interaction of Cd. Five different initial configurations (refer to Fig. 2) were considered as shown in Fig. 2. Table I reports the final configuration together with relative association energies and the Bader charge on Cd atom in the relaxed structure. The most stable site for the exohedral adsorption of Cd is 66. The association energy calculated for this site is −0.15 eV again showing the weak adsorption. The Bader charge analysis shows that the electronic configuration of Cd is unaltered. Recently, Sankar De *et al.*[19] have studied the adsorption of different elements in the periodic table and reported the most stable sites for trapping. The lowest energy configuration found for Cd in their study is "bridge site" and they define this site as an atom on the C−C bond. Importantly, there are two possible C−C bonds [66 and 65] present in the C_{60}. Nevertheless, the difference in the energy between 66 and 65 is only 0.04 eV. Furthermore, they did not consider the dispersion correction and further report only the relative energies. Therefore, we are unable to compare the association energy of Cd with their value.

C. Structure and electronic properties of B, Si, and N doped C_{60}

In order to improve the trapping of Cd at both inner and outer surfaces of the C_{60}, B, Si, and N were substitutionally doped. The optimised structures of doped C_{60} are shown in Fig. 3(a). As discussed earlier, there are two types of C−C bonds, the C−C and the C=C present in undoped C_{60} with the bond distances of 1.45 Å and 1.40 Å, respectively.

In the relaxed structure of C_{60} doped with B, B−C bond lengths [see Fig. 3(b)] are ∼0.1 Å longer than the C−C bond lengths in the pristine C_{60} and are in good agreement with the values calculated by Bai *et al.*[38] Also, there is a slight change in the C−C bond distances closer to the B. The Bader charge analysis shows that the boron donates its three outer electrons ($2s^2 2p^1$) to the nearest neighbour carbon atoms

TABLE II. Encapsulation energies of Cd incorporation inside the doped C_{60} and Bader charge on Cd.

Doped C_{60}	Encapsulation energy (eV)	Bader charge on Cd (|e|)
B·C59	−0.23	+0.21
Si·C59	−0.25	+0.20
N·C59	−0.18	+0.21

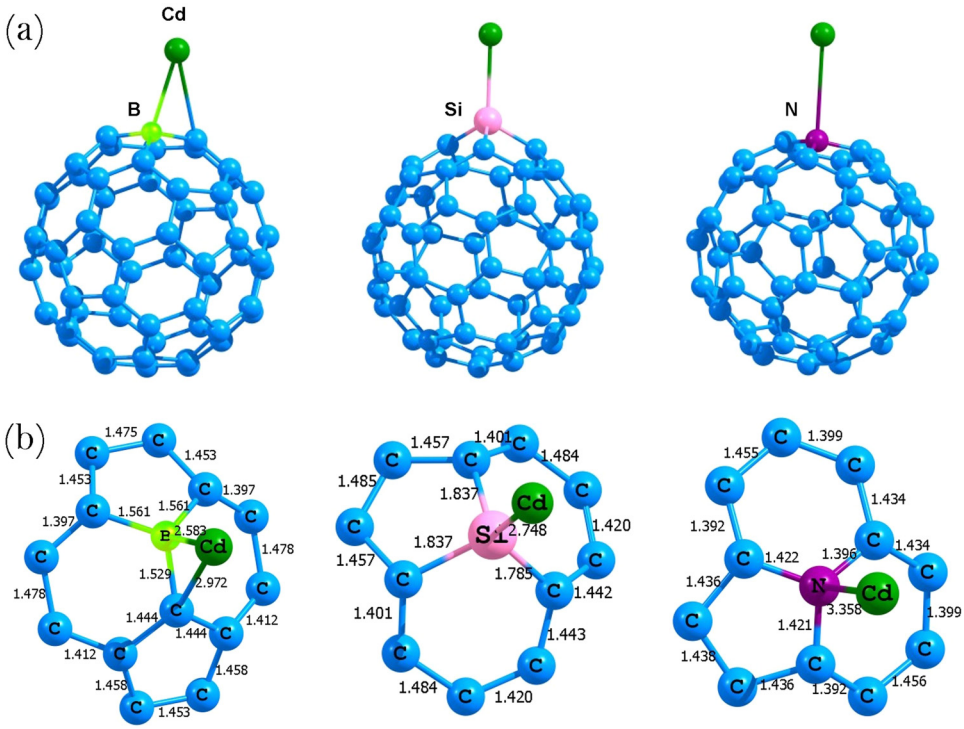

FIG. 6 (a) Relaxed structures of Cd absorbed on doped C_{60} and (b) C–X and Cd–X (X = B, Si, and N) distances.

[see Fig. 3(c)] and becomes 3+ charge. The total DOS [see Fig. 4(a)] shows that doping with B introduces additional bands just above the HOMO of C_{60} and the bandgap is reduced by 0.55 eV. The HOMO is mainly dominated by p-orbitals of B as shown in Figs. 4(b) and 5(a).

Silicon forms an outward relaxation with Si—C bond lengths between 1.79 and 1.84 Å, similar values obtained for Si substitutional doping in nanotubes[39] and fullerenes.[38] Silicon donates ~3.50 electron to the nearest neighbour carbon atoms as shown in Fig. 3(c). The total DOS [see Fig. 4(a)] shows that the HOMO is dominated by valence p orbitals of C and Si as evidenced by DOS plotted for p states of Si. The longer Si—C distances show that Si forms a single covalent bond with C and there is a vacant orbital available on Si for further bonding. This is reflected in the LUMO shown in Fig. 5(b). Doping with Si reduces the HOMO-LUMO gap by 0.45 eV.

The opposite effect is observed for nitrogen. As nitrogen is more electronegative than carbon, N gains ~2.60 electron from its nearest neighbour C atoms [see Barder charge approximation in Fig. 3(c)]. There is a slight reduction in the bond distances (~0.03 Å). The Fermi energy is shifted to the higher values.

Next, we calculated the substitutional doping energy by the following reaction:

$$E(C_{60}) + E(X) \rightarrow E(XC_{59}) + E(C), \quad (2)$$

where $E(C_{60})$ is the total energy of C_{60}, $E(X)$ is the energy of isolated dopant atom, $E(XC_{59})$ is the total energy of doped C_{60}, and $E(C)$ is the energy of isolated C atom. Calculated substitutional doping energies for B, Si, and N are 0.37 eV, 1.18 eV, and 3.09 eV, respectively. This indicates that the B-doping is the lowest energy doping strategy.

D. Encapsulation of Cd within B, Si, and N doped C_{60}

Thereafter, we calculated the encapsulation energy of Cd in the doped C_{60}. The encapsulation energies and the Bader charge on Cd are reported in Table II. In all three relaxed structures, Cd occupied closer to the centre of the cage. There is a slight enhancement in the encapsulation in B and Si doped C_{60} as evidenced by the Bader charge. This is due to the structural change in the cage by doping. Nitrogen shows almost encapsulation energy calculated with pristine C_{60}.

Table III. Association energies of Cd interacting outer surface of doped C_{60} and Bader charge on Cd and dopants.

Doped C_{60}	Association energy (eV)	Bader charge on Cd (|e|)	Bader charge on dopants (|e|)
B·C59	−0.51	+0.28	+3.00
Si·C59	−0.61	+0.20	+2.34
N·C59	−0.10	+0.02	−2.69

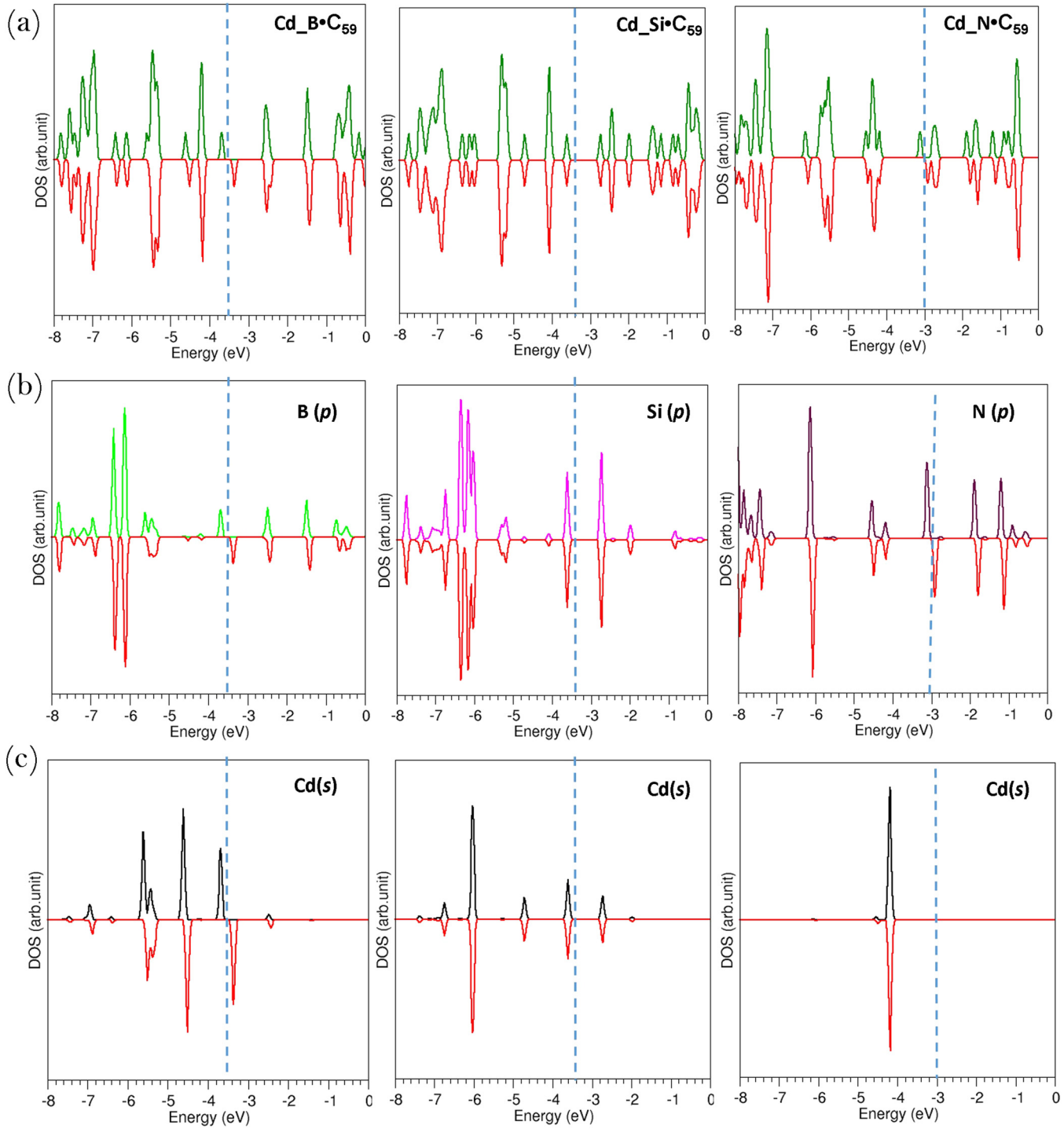

FIG. 7. (a) Total densities of states of Cd interacting doped C_{60} and (b) *p* states of doped atoms, and (c) *s* states of Cd. The vertical dotted lines correspond to the Fermi energy level.

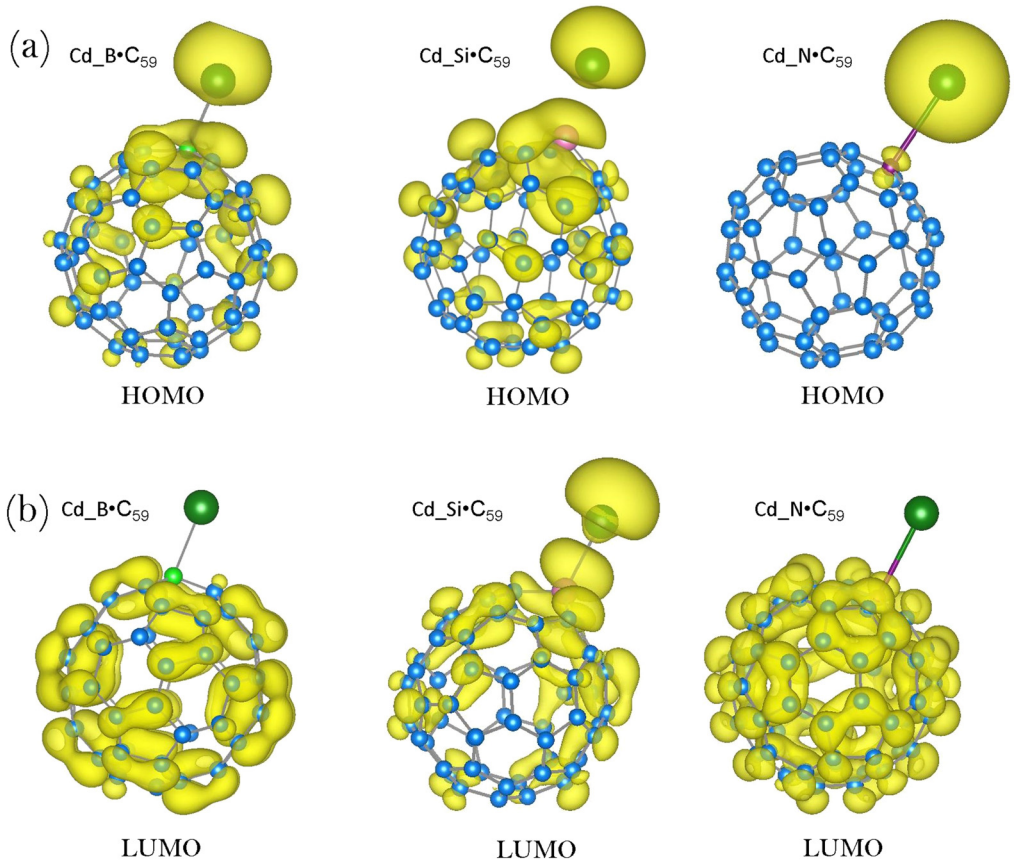

FIG. 8. (a) HOMO and (b) LUMO iso-surface charge densities calculated for Cd interacting C_{60} doped with B, Si, and N.

E. Trapping of Cd on the surface of doped C_{60}

Finally, we have considered the interaction of Cd on the surface of doped C_{60}. Different initial configurations were considered placing Cd at different positions above the dopant. However, all configurations preferred only one stable structure in each case and the final configurations are shown in Fig. 6.

Both B and Si exhibit stronger attraction with Cd. The association energies (see Table III) indicate that the trapping capability of C_{60} doped with B or Si is approximately three times stronger than the pristine C_{60}. This is due to the polarisation of positively charged B or Si with closed shell $d^{10}s^2$ configuration of Cd. This is further evidenced by the Bader charges on Cd and dopants. In the case of N, there is a repulsion between electrons localised on N and the closed shell configuration of Cd. This is further evidenced by the longer N—Cd bond length.

Total DOS's and atomic dos's for dopants and Cd are given in Fig. 7. Top of the valence band calculated for Cd interacting B doped C_{60} is a mixture of *p*-states of B and *s*-states of Cd. This is further supported by the HOMO [refer to Fig. 8(a)]. This is also the case for Cd interacting with Si doped C_{60} as evidenced by its DOS and the HOMO. In the case of Cd interacting N doped C_{60}, s states of Cd are not contributed to the HOMO (refer to Fig. 8 and DOS in Fig. 7).

IV. CONCLUSIONS

Using the density functional theory together with a dispersion correction and vdW forces, we have investigated the capacity of C_{60} and B-, Si-, and N-doped C_{60} to trap cadmium. The present calculations show that Cd is weakly trapped via van der Waals forces by C_{60} both endohedrally and exohedrally. Both B and Si doped C_{60} enhance the Cd encapsulation (trapping inside) slightly. However, significant enhancement in Cd trapping was observed on the outer surface of B and Si doped due to the attractive interaction with positively charged dopants and Cd. As the lowest substitutional energy is calculated for B, we conclude that B-doped C_{60} is the candidate material for the removal of Cd and experimental investigations should further confirm this.

ACKNOWLEDGMENTS

Computational facilities and support were provided by the High Performance Computing Centre at Imperial College London.

The authors declare that there is no competing financial interest.

REFERENCES

[1]M. Jaishankar, T. Tseten, N. Anbalagan, B. B. Mathew, and K. N. Beeregowda, Interdiscip. Toxicol. **7**, 60–72 (2014).
[2]L. Järup, Brit. Med. Bull. **68**, 167–182 (2003).
[3]E. K. Leffel, C. Wolf, A. Poklis, and K. L. White, Toxicology **188**, 233–250 (2003).
[4]S. Guan, T. Palermo, and J. Meliker, Int. J. Hyg. Envir. Heal. **218**, 147–152 (2015).
[5]N. Johri, G. Jacquillet, and R. Unwin, BioMetals **23**, 783–792 (2010).
[6]M. Tellez-Plaza, M. R. Jones, A. Dominguez-Lucas, E. Guallar, and A. Navas-Acien, Curr. Atheroscler. Rep. **15**, 356 (2013).
[7]W. Wang and V. Fthenakis, J. Hazard. Mater. **125**, 80–88 (2005).
[8]M. K. Jha, V. Kumar, J. Jeong, and J.-c. Lee, Hydrometallurgy **111–112**, 1–9 (2012).
[9]J. Nakajima, M. Fujinami, and K. Oguma, Anal. Sci. **20**, 1733–1736 (2004).
[10]P. Abiman, G. G. Wildgoose, A. Crossley, and R. G. Compton, Electroanalysis **21**, 897–903 (2009).
[11]M. A. Barakat, Arab. J. Chem. **4**, 361–377 (2011).
[12]M. Karnib, A. Kabbani, H. Holail, and Z. Olama, Energ. Procedia **50**, 113–120 (2014).
[13]X. Wang, R. Qu, J. Liu, Z. Wei, L. Wang, S. Yang, Q. Huang, and Z. Wang, Environ. Pollut. **208**, 732–738 (2016).
[14]M. R. Panuccio, A. Sorgonà, M. Rizzo, and G. Cacco, J. Environ. Manage. **90**, 364–374 (2009).
[15]J.-S. Chang, R. Law, and C.-C. Chang, Water Res. **31**, 1651–1658 (1997).
[16]H. Dai, Acc. Chem. Res. **35**, 1035–1044 (2002).
[17]Y. Wang, D. Tománek, and R. S. Ruoff, Chem. Phys. Lett. **208**, 79–85 (1993).
[18]N. Kuganathan, A. K. Arya, M. J. D. Rushton, and R. W. Grimes, Carbon **132**, 477–485 (2018).
[19]D. Sankar De, J. A. Flores-Livas, S. Saha, L. Genovese, and S. Goedecker, Carbon **129**, 847–853 (2018).
[20]E. Brocławik and A. Eilmes, J. Chem. Phys. **108**, 3498–3503 (1998).
[21]K. Kikuchi, K. Kobayashi, K. Sueki, S. Suzuki, H. Nakahara, Y. Achiba, K. Tomura, and M. Katada, J. Am. Chem. Soc. **116**, 9775–9776 (1994).
[22]S. K. Saha, D. P. Chowdhury, S. K. Das, and R. Guin, Nucl. Instrum. Methods Phys. Res. Sect. B **243**, 277–281 (2006).
[23]A. K. Srivastava, S. K. Pandey, and N. Misra, Mater. Chem. Phys. **177**, 437–441 (2016).
[24]J. Lu, Y. Zhou, X. Zhang, and X. Zhao, Mol. Phys. **99**, 1199–1202 (2001).
[25]S. C. Cho, T. Kaneko, H. Ishida, and R. Hatakeyama, J. Appl. Phys. **117**, 123301 (2015).
[26]H. Minezaki, K. Oshima, T. Uchida, T. Mizuki, R. Racz, M. Muramatsu, T. Asaji, A. Kitagawa, Y. Kato, S. Biri, and Y. Yoshida, Nucl. Instrum. Methods Phys. Res. Sect. B **310**, 18–22 (2013).
[27]N. Kuganathan, J. C. Green, and H.-J. Himmel, New J. Chem. **30**, 1253–1262 (2006).
[28]J. R. Heath, S. C. O'Brien, Q. Zhang, Y. Liu, R. F. Curl, F. K. Tittel, and R. E. Smalley, J. Am. Chem. Soc. **107**, 7779–7780 (1985).
[29]G. Kresse and J. Furthmüller, Phys. Rev. B **54**, 11169–11186 (1996).
[30]G. Kresse and D. Joubert, Phys. Rev. B **59**, 1758–1775 (1999).
[31]J. P. Perdew, K. Burke, and M. Ernzerhof, Phys. Rev. Lett. **77**, 3865–3868 (1996).
[32]W. H. Press, S. A. Teukolsky, W. T. Vetterling, and B. P. Flannery, *Numerical Recipes in C: The Art of Scientific Computing*, 2nd ed. (Cambridge University Press, 1992).
[33]S. Grimme, J. Antony, S. Ehrlich, and H. Krieg, J. Chem. Phys. **132**, 154104 (2010).
[34](a) P. Varotsos, J. Appl. Phys. **101**, 123503 (2007); (b) A. Chroneos and R. V. Vovk, Solid State Ion. **274**, 1–3 (2015); (c) A. Chroneos, Appl. Phys. Rev. **3**, 041304 (2016).
[35]J. M. Hawkins, Acc. Chem. Res. **25**, 150–156 (1992).
[36]J. Goclon, K. Winkler, and J. T. Margraf, RSC Adv. **7**, 2202–2210 (2017).
[37]G. Henkelman, A. Arnaldsson, and H. Jónsson, Comput. Mater. Sci. **36**, 354–360 (2006).
[38]H. Bai, W. Ji, X. Liu, L. Wang, N. Yuan, and Y. Ji, J. Chem. **2013**, 9 (2013).
[39]R. J. Baierle, S. B. Fagan, R. Mota, A. J. R. da Silva, and A. Fazzio, Phys. Rev. B **64**, 085413 (2001).